

## ARTICLES

## Temperature and Size Dependence of Nonradiative Relaxation and Exciton–Phonon Coupling in Colloidal CdTe Quantum Dots

G. Morello,\*† M. De Giorgi,† S. Kudera,† L. Manna,† R. Cingolani,† and M. Anni‡

Distretto Tecnologico ISUFI and Dipartimento di Ingegneria dell'Innovazione, National Nanotechnology Laboratory (NNL) of CNR-INFM, Università degli Studi di Lecce, Via per Arnesano 73100 Lecce, Italy

Received: December 4, 2006; In Final Form: February 6, 2007

We report on the temperature and size dependence of the photoluminescence of core CdTe colloidal quantum dots (QDs). We show that at temperatures lower than 170 K a thermally activated transition between two different states separated by about 12–20 meV takes place. At temperatures higher than 170 K, the main nonradiative process is thermal escape assisted by multiple longitudinal optical (LO) phonons absorption. Moreover, we show that quantum confinement affects both the exciton–acoustic phonons and the exciton–LO phonons coupling. The coupling constant with acoustic phonons is strongly enhanced in QDs (up to  $31\mu\text{eV/K}$ ) with respect bulk CdTe ( $0.7\mu\text{eV/K}$ ). On the contrary, the exciton-LO phonons coupling constant decreases as the dot size decreases (down to 14 meV with respect 24.5 meV in the bulk).

## I. Introduction

Semiconductor nanocrystals have attracted considerable interest in the last years, because of their potential applications to light emitting diodes (LEDs),<sup>1,2</sup> photovoltaic cells,<sup>3</sup> and optically pumped lasers.<sup>4</sup> Colloidal semiconductor quantum dots (QDs) have been also coupled to biological molecules such as proteins and DNA.<sup>5,6</sup> These QDs bioconjugates can be used as biomedical fluorescence labels for investigating biomolecular interactions and developing high-sensitivity detection and imaging systems.<sup>5,6</sup> Nowadays, advanced colloidal synthesis techniques allow the growth of highly monodispersed<sup>7</sup> II–VI QDs with high-photoluminescence (PL) quantum yield.<sup>8,9</sup> A detailed study of the QDs photophysics with a particular attention to nonradiative processes is not only interesting for fundamental physics, but it is also relevant to the exploitation of nanocrystals in practical applications. To date, several relaxation processes have been proposed to explain the photophysics of CdSe QDs, including the thermally activated exciton transition from dark to bright states<sup>10</sup> and carriers surface localization in trap states.<sup>11</sup> Moreover, it has been shown that at room temperature the main nonradiative process in CdSe/ZnS core/shell QDs is thermal escape, assisted by multiple longitudinal optical (LO) phonons absorption,<sup>12</sup> while at low temperature evidence for carrier trapping at surface defects was found. Despite these results, the role and the chemical origin<sup>37</sup> of the surface defect states in the radiative and nonradiative relaxation in nanocrystals has not been clarified completely. The existence of surface states due to unpassivated dangling bonds has been invoked to explain anomalous red-shifted emission bands in colloidal nanocrystals.

On the contrary, it has been recently shown that above-gap trap states<sup>13</sup> affect the ultrafast relaxation dynamics<sup>14</sup> and the single nanoparticle PL spectra of CdSe quantum rods<sup>15</sup> due to charge trapping and local electric field fluctuations. These effects are expected to be dependent on the chemical composition of the QDs on the density of surface defects and on the nanocrystals size.

In this work, we performed a detailed analysis of the PL temperature dependence of colloidal CdTe core QDs with diameters varying between 4.2 and 5.9 nm. We found that the QDs PL is due to a thermally activated transition between two different states at low temperatures.

Moreover, we investigated the size dependence of the coupling with both acoustical and optical phonons. We show that the acoustic phonons coupling constant is strongly increased, up to  $31\mu\text{eV/K}$  with respect to the bulk CdTe ( $0.7\mu\text{eV/K}$ ). On the other hand, the LO phonons coupling constant is reduced down to 14 meV for the smallest dots with respect to the bulk (24.5 meV). We show that the main nonradiative process affecting the PL quantum yield at high temperature is thermal escape assisted by multiple LO phonons absorption. The average number of phonons assisting the thermal escape increases from 4 for the 5.9 nm diameter dots up to 6 for the 4.2 nm ones, which is in quantitative agreement with the increased energy splitting occurring in the smaller dots.

## II. Experiment

We prepared CdTe QDs of different sizes, following the method described in ref 16. The average diameter of the dots was estimated by TEM measurements to be 4.2, 4.9, and 5.9 nm for samples A1, A2, and A3, respectively. The QDs have been deposited by drop casting from chloroform solution on Si–SiO<sub>2</sub> substrates. For each sample, we performed PL measurements in the temperature range of 15 ÷ 300 K in steps of

\* Corresponding author. E-mail address: giovanni.morello@unile.it. Alternate address: ISUFI + Institute for Advanced Interdisciplinary Studies, Università degli Studi di Lecce, Via per Arnesano 73100 Lecce, Italy.

† Distretto Tecnologico ISUFI.

‡ Dipartimento di Ingegneria dell'Innovazione.

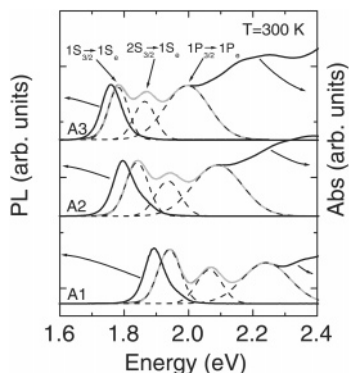


**Figure 1.** Room-temperature absorption and PL spectra of the investigated samples in chloroform solutions (black lines) and best fit Gaussians (gray lines).

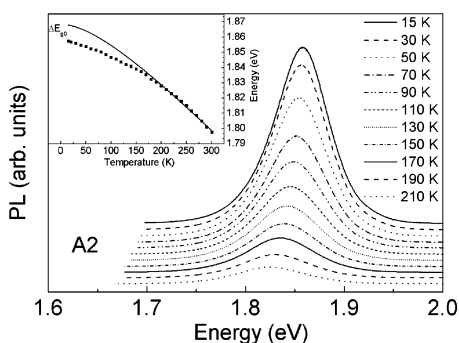


**Figure 2.** PL spectra as a function of temperature for sample A2. Inset: experimental energy gap for the same sample (full squares), and best fit curve (continuous line).

10 K. The samples were excited by ion Argon laser ( $\lambda = 458$  nm). The sample emission was dispersed by a monochromator (0.32 m focal length) and detected by a Si-CCD camera. The PL measurements were performed in vacuum in a closed-cycle He cryostat. The absorption spectra were measured in solution with a spectrophotometer.

### III. Results and Discussion

The absorption spectra of the QDs at room temperature (see Figure 1) show several peaks, corresponding to different optical transitions. The first three resonances can be reproduced by the superposition of three Gaussian bands (see Figure 1). The best fit peak energies clearly show the blue-shift of the first absorption peak and the increase of the energy splitting among the confined states, as the dots size decreases. The three first absorption peaks are due to  $1S_{3/2} \rightarrow 1S_e$ ,  $2S_{3/2} \rightarrow 1S_e$ , and  $1P_{3/2} \rightarrow 1P_e$  transitions.<sup>17,18</sup>

A typical temperature dependence of the PL spectra is reported in Figure 2, for sample A2. The spectra exhibit a weak low-energy tail (not visible in solution) that can be assigned to emission from the larger dots in the size distribution, enhanced by Förster transfer (FRET)<sup>19</sup> from the smaller dots. As the temperature increases, the PL spectra show a red-shift of the peak energy, increasing broadening and decreasing intensity.

In semiconductor nanostructures, the temperature dependence of the energy gap is usually similar to the bulk semiconductor one,<sup>20–22</sup> except for a temperature-independent energy off-set due to the quantum confinement. The experimental PL temperature dependence is thus well reproduced by the Varshni relation

$$E_g(T) = E_{g0} - \alpha \frac{T^2}{(T + \beta)} \quad (1)$$

with  $\alpha$  and  $\beta$  consistent with the bulk values. In eq 1,  $E_{g0}$  is the energy gap at 0 K,  $\alpha$  is the temperature coefficient, and the value of  $\beta$  is close to the Debye temperature  $\theta_D$  of the material. On the other hand, the experimental PL peak energy temperature dependence cannot be reproduced by the Varshni relation with “bulk-like”  $\alpha$  and  $\beta$  when transitions between different states take place in the investigated temperature range.<sup>10,11</sup> In our case the experimental data can be fitted to eq 1 with  $\alpha$  and  $\beta$  values consistent with bulk CdTe only for  $T \geq 150$ – $170$  K, while a weaker temperature dependence is present at low temperature. Values of  $\alpha$  and  $\beta$  not consistent with CdTe are instead obtained by all the data or only the  $T \leq 150$  K ones. Keeping  $\beta$  fixed<sup>24</sup> at the bulk value<sup>22</sup> of 158 K we find a best fit value for  $\alpha = 3.2 \times 10^{-4}$  eV/K very close to the bulk value ( $3 \times 10^{-4}$  eV/K) reported in literature.<sup>23</sup> For temperatures below 170 K, the experimental emission energy is lower than the extrapolated value of the  $T \geq 170$  K best fit curve with a maximum difference  $\Delta E_{g0}$  at 15 K of the order of 12–20 meV in the three samples. We observe that for all the samples, the experimental data follow a bulklike best fit curve for  $k_B T \geq \Delta E_{g0}$  (where  $k_B$  is the Boltzmann constant) suggesting that a thermally activated transition between two different states energetically separated by  $\Delta E_{g0}$ , takes place. This transition could be due to different possible processes, like the dark-bright exciton transition,<sup>10</sup> or the transitions between intrinsic and surface states, such as detrapping from surface trap states to intrinsic electronic states,<sup>11</sup> or transition from intrinsic states to higher energy-localized surface states.<sup>14</sup> The dark-bright exciton transition can be ruled out as the typical activation energies<sup>25</sup> are much smaller than the  $\Delta E_{g0}$  values (typically a few meV) and are strongly size dependent, whereas in our case  $\Delta E_{g0}$  does not show any regular variation with the QDs size (see Table 1). This suggests that a thermally activated transition involving surface and core states is responsible for the PL peak temperature dependence. Moreover, the Stokes shift at room temperature shows an expected increase by decreasing size<sup>26</sup> (see Figure 1): 24 meV, 42 meV, and 52 meV for sample A3, A2, and A1, respectively. This trend suggests that the nature of the emitting state at room temperature is intrinsic.

To determine the different nonradiative processes affecting carriers relaxation, we studied the PL intensity variations with temperature. In Figure 3 we show the PL intensity dependence on  $1/k_B T$ . For all the samples, the photoluminescence intensity is almost constant up to about 40 K, while a first thermally activated PL decrease is visible in the range 40–170 K, followed by a stronger exponential decrease up to 300 K. In general, the relaxation processes in QDs include radiative relaxation, Auger nonradiative scattering,<sup>27,28</sup> Förster energy transfer between dots of different dimensions, thermal escape from the dot,<sup>31</sup> and carriers localization at surface states.<sup>32,33</sup> In our excitation regime (few W cm<sup>-2</sup>) the Auger interaction can be neglected, as the average excitation per dot is ( $N_0 \ll 1$ ).<sup>34</sup> Moreover, FRET can be neglected because we do not observe significant differences between the PL spectra obtained from liquid and solid samples.

Assuming a temperature-independent radiative lifetime due to the strong confinement regime,<sup>29</sup> the temperature dependence of the PL intensity, taking into account the radiative relaxation, a thermally activated nonradiative process (with activation energy  $E_a$ ),<sup>30</sup> and the thermal escape is given by<sup>12</sup>

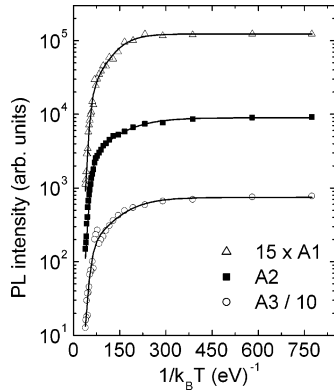


**Figure 3.** Integrated PL intensity dependence on the samples' temperature (symbols) and best fit curves (continuous lines) to eq 3. The data are scaled for clarity.

$$I_{\text{PL}}(T) = \frac{I_0}{1 + a(e^{-E_a/k_B T}) + b(e^{E_{\text{LO}}/k_B T} - 1)^{-m}} \quad (2)$$

where  $I_{\text{PL}}(T)$  is the integrated PL intensity at temperature  $T$ ,  $I_0$  is the 0 K integrated PL intensity, and  $m$  is the number of LO phonons involved in thermal escape of carriers and  $E_{\text{LO}}$  is their energy.<sup>35</sup> The best fit parameters are reported in Table 1.

We observe that the best fit value of  $E_a$  is, for all the samples, very similar to the  $\Delta E_{g0}$  values extracted from the PL peak energy analysis. This suggests that the low-temperature PL quenching process is due to the same thermally activated transition between intrinsic and defect states that affect the PL peak temperature dependence. In epitaxial QDs, simultaneous presence of an anomalous energy gap temperature dependence and of a PL quenching process with an activation energy of a few tens of meV is typical of transitions between intrinsic and defect states.<sup>36</sup> In colloidal nanocrystals, some experiments on CdTe and CdSe QDs showed the presence of emitting surface states lying several tens of meV below the band edge emission,<sup>37,38</sup> while theoretical results on potentially emitting surface defect states that resonant with or at higher energy than the band edge are also present.<sup>13</sup> However, the exact chemical origin of these surface states is not yet known.<sup>37</sup> Our results can be due to a thermally induced detrapping from a surface defect state to a weakly radiatively coupled intrinsic state or to an unusual thermally activated trapping. Further experiments, like time-resolved PL, have to be performed to attribute our results to trapping or detrapping. Another possible process can be a thermally activated exciton migration from larger to smaller dots.<sup>39</sup> However, this process is unlikely because the average distance between different QDs in our samples is of the order of microns, too large to permit efficient FRET from small to large dots. At  $T \geq 170$  K, we observe a thermal escape process, where the average number of LO phonons absorbed in the process clearly increases as the dot diameter decreases from about 4 to about 6. This is consistent with the increasing energy difference between adjacent states due to the stronger confinement of smaller dots, which leads to an increase of the energy that a carrier has to absorb to jump from one state to the following one. To confirm this conclusion, a quantitative comparison between the total energy absorbed from the LO phonons in the thermal escape given by  $E_{\text{escape}} = m(E_{\text{LO}})$  and the energy difference between the excited states involved in the process is required. First of all, we remember that the thermal escape mainly involves the carrier with the smallest energy difference between consecutive confined state, which in our case is the hole, due to its higher effective mass.<sup>23</sup> Moreover, as shown in Figure 1, the two first absorption peaks are due to

**TABLE 1: Best Fit Values of the Activation Energy  $E_a$  of the Low-Temperature Quenching Process and of the Number  $m$  of LO Phonons Absorbed in the Thermal Escape<sup>a</sup>**

sample	$E_a$ (meV)	$m$	$\Delta E_{g0}$ (meV)	$E_{\text{LO}}$ (meV)	$\Delta E_{1,2}$ (meV)	$E_{\text{escape}}$ (meV)
A1	$23.5 \pm 2.0$	$5.6 \pm 1.7$	21	$20 \pm 5$	124.5	$110 \pm 30$
A2	$13.6 \pm 0.7$	$4.9 \pm 0.2$	12	$19.1 \pm 1.5$	96.5	$94 \pm 4$
A3	$15.6 \pm 1.7$	$4.0 \pm 0.3$	17	$22 \pm 4$	82.2	$92 \pm 7$

<sup>a</sup>  $\Delta E_{1,2}$  is the energy difference between the two first absorption peaks, while  $E_{\text{escape}} = m(E_{\text{LO}})$ . The values of  $E_{\text{LO}}$  and  $\Delta E_{g0}$  are also reported for clarity.

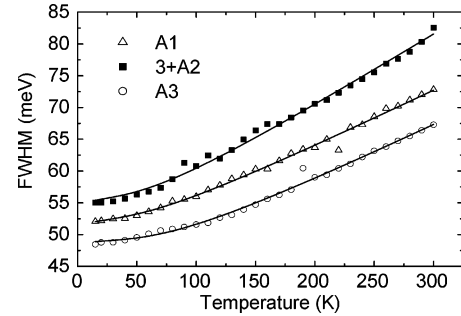


**Figure 4.** The fwhm of the PL spectra as a function of temperature (symbols) for the three samples and respective best fit curves (continuous lines). The data of the sample A2 are vertically translated by 3 meV for clarity.

**TABLE 2: Best Fit Values of  $\sigma$ ,  $\Gamma_{\text{LO}}$ , and  $E_{\text{LO}}$  for the Three Samples**

sample	$\sigma$ ( $\mu\text{eV/K}$ )	$\Gamma_{\text{LO}}$ (meV)	$E_{\text{LO}}$ (meV)
A1	$31 \pm 7$	$14 \pm 3$	$20 \pm 5$
A2	$33 \pm 6$	$18.3 \pm 0.9$	$20 \pm 1.5$
A3	$14 \pm 5$	$21 \pm 4$	$22 \pm 4$

$1S_{3/2} \rightarrow 1S_e$  and  $2S_{3/2} \rightarrow 1S_e$  transitions.<sup>17,18</sup> This allows us to estimate the energy difference between the  $1S_{3/2}$  and the  $2S_{3/2}$  hole states simply as the difference between the first two absorption peaks energies ( $\Delta E_{1,2}$  in Table 1). From the comparison of  $\Delta E_{1,2}$  with  $E_{\text{escape}} = m(E_{\text{LO}})$  (see Table 1), we observe an overall very good agreement for all the samples, suggesting that the thermal escape involves hole states.

Finally, to study the size dependence of exciton–phonon coupling, we analyzed the temperature dependence of the PL broadening obtained from the Gaussian deconvolution. The experimental values of the PL spectrum Full Width at Half-Maximum (FWHM) (see Figure 4), obtained from a Gaussian best fit of the spectra, clearly show that the FWHM increases with the temperature. As the PL broadening is partially inhomogeneous and partially homogeneous, because of exciton–phonons scattering, we fitted the experimental FWHM to the following equation:<sup>40</sup>

$$\Gamma(T) = \Gamma_{\text{inh}} + \sigma T + \Gamma_{\text{LO}}(e^{E_{\text{LO}}/k_B T} - 1)^{-1} \quad (3)$$

Here,  $\Gamma_{\text{inh}}$  is the inhomogeneous broadening, which is temperature independent, and it is due to fluctuations in size, shape, and composition of the nanocrystals,  $\sigma$  is the exciton–acoustic phonons coupling coefficient,  $\Gamma_{\text{LO}}$  represents the exciton–LO phonons coupling coefficient,  $E_{\text{LO}}$  is the LO phonon energy, and  $k_B$  is the Boltzmann constant. In all the investigated samples, the best fit curve well reproduces the experimental data for the best fit parameters reported in Table 2.

We observe that the best fit values of the exciton–acoustic phonons coupling constant  $\sigma$  are about 3 orders of magnitude

higher than the theoretical value estimated by Rudin et al.<sup>41</sup> (about 0.72  $\mu\text{eV/K}$ ) for bulk CdTe. This result is consistent with the theoretical prediction of a strong increase of the coupling with acoustic phonons in zero-dimensional systems.<sup>12</sup> Moreover, our results are also in qualitative agreement with the increase of the acoustic phonons coupling with the increasing two-dimensional confinement observed in CdTe quantum wells.<sup>42</sup> Despite this qualitative agreement, we observe that the  $\sigma$  value, which determines the low-temperature broadening increase, could be affected by the intrinsic-defects state transition that takes place below 170 K. On the contrary, the best fit values of the carrier-LO phonons coupling coefficient  $\Gamma_{\text{LO}}$ , obtained in a temperature range where the emission is intrinsic, is smaller than the theoretical bulk value<sup>41</sup> ( $\Gamma_{\text{LO}} = 24.5$  meV) and decreases as the QDs size decreases. This result can also be ascribed to quantum confinement, and it is consistent with theoretical prediction and experimental observation.<sup>12,43,44</sup> Finally, we did not find any dependence on the quantum confinement for the LO phonon energy, as reported in literature,<sup>45</sup> but its value is within the fitting error consistent with the bulk value (21.1 meV<sup>23</sup>).

#### IV. Conclusions

In conclusion, we studied the temperature and size dependence of the PL spectra in colloidal CdTe core QDs. We demonstrated that at temperatures lower than about 150–170 K a thermally activated transition between two different states separated by about 12–20 meV takes place.

We demonstrated that at higher temperature, the main nonradiative process that limits the quantum efficiency is thermal escape, induced by multiphonon absorption. The number  $m$  of phonons involved in the process is dependent on the dots size and varies from 4, in smallest dots, to about 6 for the largest ones. Finally, we have studied the size dependence of the exciton–phonons coupling. We found that it is strongly dependent on the quantum confinement. In particular, the coupling with acoustic phonons increases with respect bulk material, and the exciton–optical phonons coupling increases in larger dots.

#### References and Notes

- (1) Coe, S.; Woo, W. K.; Bawendi, M. G.; Bulovic, V. *Nature* **2002**, *420*, 800.
- (2) Tessler, N.; Medvedev, V.; Kazes, M.; Kan, S. H.; Banin, U. *Science* **2002**, *295*, 1506.
- (3) Greenham, N. C.; Peng, X.; Alivisatos, A. P. *Phys. Rev. B* **1996**, *54*, 17628.
- (4) Klimov, V. I. *Science* **2003**, *28*, 214.
- (5) Bruchez, M., Jr.; Moranna, M.; Gin Pand Weiss, S. *Science* **1998**, *281*, 2013.
- (6) Pathak, S.; Choi, S. K.; Arnheim, N.; Thompson, M. E. *J. Am. Chem. Soc.* **2001**, *123*, 4103.
- (7) Murray, C. B.; Norris, D. J.; Bawendi, M. G. *J. Am. Chem. Soc.* **1993**, *115*, 8706.
- (8) Dabbousi, B. O.; Rodriguez-Viejo, J.; Mikulec, F. V.; Heine, J. R.; Mattoussi, H.; Ober, R.; Jensen, K. F.; Bawendi, M. G. *J. Phys. Chem. B* **1997**, *101*, 9463.
- (9) Reiss, P.; Bleuse, J.; Pron, A. *Nano. Lett.* **2002**, *2*, 781.
- (10) Crooker, S. A.; Barrick, T.; Hollingsworth, J. A.; Klimov, V. I. *Appl. Phys. Lett.* **2003**, *82*, 2793.
- (11) Lee, W. Z.; Shu, G. W.; Wang, J. S.; Shen, J. L.; Lin, C. A.; Chang, W. H.; Ruan, R. C.; Chou, W. C.; Lu, H. C.; Lee, Y. C. *Nanotechnology* **2005**, *16*, 1517.
- (12) Valerini, D.; Cretù, A.; Lomascolo, M.; Manna, L.; Cingolani, R.; Anni, M. *Phys. Rev. B* **2005**, *71*, 235409.
- (13) Bawendi, M. G.; Carrol, P. J.; Wilson, W. L.; Brus, L. E. *J. Chem. Phys.* **1992**, *96*, 946.
- (14) Cretù, A.; Anni, M.; Zavelani Rossi, M.; Lanzani, G.; Leo, G.; Della Sala, F.; Manna, L.; Lomascolo, M. *Phys. Rev. B* **2005**, *72*, 125346.
- (15) Rothenberg, E.; Kazes, M.; Shaviv, E.; Banin, U. *Nano Lett.* **2005**, *5*, 1581.
- (16) Peng, Z. A.; Peng, X. G. *J. Am. Chem. Soc.* **2001**, *123*, 183.
- (17) Richard, T.; Lefebvre, P.; Mathieu, H.; Allegre, J. *Phys. Rev. B* **1996**, *53*, 7287.
- (18) Efros, Al. L.; Rosen, M. *Phys. Rev. B* **1998**, *58*, 7120.
- (19) Kagan, C. R.; Murray, C. B.; Bawendi, M. G. *Phys. Rev. B* **1996**, *54*, 8633.
- (20) Tarì, D.; De Giorgi, M.; Cingolani, R.; Foti, E.; Coriasso, C. *J. Appl. Phys.* **2005**, *97*, 043705.
- (21) Brusafoni, L.; Sanguinetti, S.; Grilli, E.; Guzzi, M.; Bignazzi, A.; Bogani, F.; Carraresi, L.; Colocci, M.; Bosacchi, A.; Frigeri, P.; Franchi, S. *Appl. Phys. Lett.* **1996**, *69*, 3354.
- (22) Pal, U.; Herrera Pérez, J. L.; Piqueras, J.; Dieguéz, E. *Mater. Sci. Eng., B* **1996**, *42*, 297.
- (23) *Landolt-Börnstein Numerical Data and Functional Relationship in Science and Technology*, Group II–VI; Hellwege, K. H.; ed.; Springer-Verlag: Berlin, Germany, 1982; Vol. 17a.
- (24) The best fit is performed in a temperature range in which  $E_g(T)$  is weakly dependent on  $\beta$  and it is mainly dependent on  $\alpha$ . This prevents the extraction of accurate best fit values of  $\beta$  by leaving it free in the fitting session.
- (25) Efros, Al. L.; Rosen, M.; Kuno, M.; Nirmal, M.; Norris, D. J.; Bawendi, M. *Phys. Rev. B* **1996**, *54*, 4843.
- (26) Yu, Z.; Li, J.; O'Connor, D. B.; Wang, L. W.; Barbara, P. F. *J. Phys. Chem. B* **2003**, *107*, 5670.
- (27) Ghanassi, M.; Schanne-Klein, M.; Hache, F.; Ekimov, A.; Ricard, D. *Appl. Phys. Lett.* **1993**, *62*, 78.
- (28) Klimov, V. I.; McBranch, D. W. *Phys. Rev. B* **1997**, *55*, 13173.
- (29) Gotoh, H.; Ando, H.; Takagahara, T. *J. Appl. Phys.* **1997**, *81*, 1785.
- (30) The assumption of a single thermally activated process is the simplest to describe the observed exponential decrease of the PL intensity in the range 40–170 K. We observe that a similar PL temperature dependence could result also from more complicated processes, like the thermal activation of trapping in a distribution of defects at slightly different energies.
- (31) Yang, W.; Lowe-Webb, R. R.; Lee, H.; Sercel, P. C. *Phys. Rev. B* **1997**, *56*, 13314.
- (32) Klimov, V. I.; Bolivar, P. H.; Kurz, H. *Phys. Rev. B* **1996**, *53*, 1463.
- (33) Nuss, M. C.; Zinth, W.; Kaiser, W. *Appl. Phys. Lett.* **1986**, *49*, 1717.
- (34) Klimov, V. I.; McBranch, D. W.; Leatherdale, C. A.; Bawendi, M. G. *Phys. Rev. B* **1999**, *60*, 13740.
- (35) De Giorgi, M.; Ling, C.; von Plessen, G.; Feldmann, J.; De Rinaldis, S.; Passaseo, A.; De Vittorio, M.; Cingolani, R.; Lomascolo, M. *Appl. Phys. Lett.* **2001**, *79*, 3968.
- (36) Wu, Yi-hong; Arai, K.; Yao, T. *Phys. Rev. B* **1996**, *53*, R10485.
- (37) Wang, X.; Yu, W. W.; Zhang, J.; Aldana, J.; Peng, X.; Xiao, M. *Phys. Rev. B* **2003**, *68*, 125318.
- (38) Chen, W.; Joly, A. G.; McCready, D. E. *J. Chem. Phys.* **2005**, *122*, 224708.
- (39) Patané, A.; Levin, A.; Polimeni, A.; Eaves, L.; Main, P. C.; Henini, M.; Hill, G. *Phys. Rev. B* **2000**, *62*, 11084.
- (40) Lee, J.; Koteles, E. S.; Vassell, M. O. *Phys. Rev. B* **1986**, *33*, 5512.
- (41) Rudin, S.; Reinecke, T. L.; Segall, B. *Phys. Rev. B* **1990**, *42*, 11218.
- (42) Mayer, E. J.; Pelekanos, N. T.; Kuhl, J.; Magnea, N.; Mariette, H. *Phys. Rev. B* **1995**, *51*, R17263.
- (43) Gindele, F.; Hild, K.; Langbein, W.; Woggon, U. *J. Lumin.* **2000**, *87–89*, 381.
- (44) Nomura, S.; Kobayashi, T. *Phys. Rev. B* **1992**, *45*, 1305.
- (45) Trallero-Giner, C.; Debernardi, A.; Cardona, M.; Menéndez-Proupin, E.; Ekimov, A. I. *Phys. Rev. B* **1998**, *57*, 4664.